Applied Physics Letters

Size and shape evolution of embedded single-crystal α-Fe nanowires

Cite as: Appl. Phys. Lett. **87**, 203110 (2005); https://doi.org/10.1063/1.2128480
Submitted: 12 May 2005 . Accepted: 26 September 2005 . Published Online: 10 November 2005

L. Mohaddes-Ardabili, H. Zheng, Q. Zhan, S. Y. Yang, R. Ramesh, L. Salamanca-Riba, M. Wuttig, S. B. Ogale, and X. Pan

Size and shape evolution of embedded single-crystal α-Fe nanowires

L. Mohaddes-Ardabili,[a] H. Zheng, Q. Zhan, S. Y. Yang, and R. Ramesh
Department of Materials Science and Engineering and Department of Physics, University of California, Berkeley, California 94720

L. Salamanca-Riba and M. Wuttig
Department of Materials Science and Engineering, University of Maryland, College Park, Maryland 20742

S. B. Ogale
Center for Superconductivity Research, Department of Physics, University of Maryland, College Park, Maryland 20742

X. Pan
Department of Materials Science and Engineering, University of Michigan, Ann Arbor, Michigan 48109

(Received 12 May 2005; accepted 26 September 2005; published online 10 November 2005)

The size and shape evolution of embedded ferromagnetic α-Fe nanowires is discussed. The α-Fe nanowires are formed by pulsed-laser deposition of $La_{0.5}Sr_{0.5}FeO_{3-x}$ on single-crystal $SrTiO_3$ (001) substrate in reducing atmosphere. The average diameter of the nanowires increases from $d \approx 4$ to 50 nm as the growth temperature increases from $T=560$ to 840 °C. Their in-plane shape evolves from circular to octahedral and square shape with [110] facets dominating as the growth temperature increases. A fitting to a theoretical calculation shows that the circular shape is stable when the diameter of the nanowires is smaller than 8 nm. © *2005 American Institute of Physics*.
[DOI: 10.1063/1.2128480]

Ferromagnetic nanostructures have attracted considerable interest due to the variety of new materials and devices that could be developed from them such as data-storage media, spin electronics, and memory devices.[1] As the device miniaturization trend continues, new sample growth and patterning methods are needed to fabricate ferromagnetic nanostructures by efficient *in situ* growth processes that may allow the realization of length scales far below the limits of conventional photolithography.

Recently we reported a simple and novel approach to make single crystalline ferromagnetic iron nanowires by means of self-assembly in heteroepitaxial thin film.[2] The approach is based on the combination of two principles. The first is heteroepitaxy and the second is the phase control under reduction of perovskite-type oxides of general formula $LaMO_3$ where M is a group VIII metal. It has been shown[3] that these perovskite oxides in bulk form can be reduced to stable compounds having a charge of 1–3 electron per molecule with the full reduced state being the metal M in the La_2O_3 matrix (reduction of 3 electrons per molecule). Therefore, depending on the oxidation state of M, these oxides provide an interesting opportunity to create metallic or oxide nanostructures embedded in an oxide matrix through a spontaneous phase decomposition.[2,4] In addition, in the thin film processing, the nanostructure and the oxide matrix can be epitaxial with respect to each other as well as to the substrate, providing the possibility of heteroepitaxy in three dimensions (i.e., both in plane and out of plane).[5,6] In this work, we present the results of these two principles applied to a single-phase $La_{1-x}Sr_xFeO_{3-x}$ system, and specially focus on the size and shape evolution of the resulting ferromagnetic α-Fe nanowires with varying depositon temperature.

The thin films for this study were grown on single crystalline $SrTiO_3$ (001) substrates using pulsed laser deposition method with a KrF ($\lambda=248$ nm) excimer laser and a single-phase ceramic $La_{0.5}Sr_{0.5}FeO_{3-x}$ target. The films were deposited in vacuum ($<5\times10^{-6}$ Torr) at various temperatures ranging from $T=560-840$ °C and cooled in the same vacuum. The laser energy density was 1.4 J/cm^2, and the film growth rate was ~1.2 Å/s.

Figure 1(a) shows the x-ray θ-2θ diffraction spectrum of a film deposited at $T=840$ °C. The diffraction peaks can be assigned to (00ℓ) perovskite $SrTiO_3$($a=0.3905$ nm),

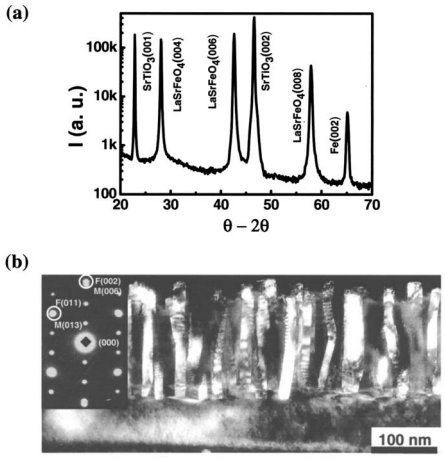

FIG. 1. (a) X-ray θ-2θ scan showing $(00l)$ families of peaks, which can be assigned to α-Fe, $LaSrFeO_4$, and the $SrTiO_3$ substrate. (b) Cross-section dark field TEM image of the added sample grown at $T=760$ °C showing α-Fe nanowires embedded in $LaSrFeO_4$ matrix. The inset shows electron diffraction pattern obtained from the film illustrating out-of-plane heteroepitaxy between $LaSrFeO_4$ and α-Fe.

[a]Author to whom correspondence should be addressed; also at: Department of Materials Science and Engineering, University of Maryland at College Park; electronic mail: ladan@berkeley.edu

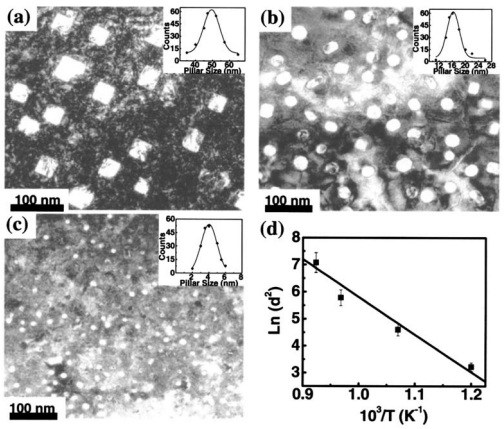

FIG. 2. Plan view TEM image of the film grown at (a) $T=840\ ^\circ\mathrm{C}$, (b) $T=760\ ^\circ\mathrm{C}$, and (c) $T=560\ ^\circ\mathrm{C}$. The inset in all figures shows the statistical lateral size distribution of the pillars. (d) Arrhenius fit of the lateral dimension of the α-Fe nanowires as a function of growth temperature.

$(00\ell)\mathrm{LaSrFeO_4}$ ($a=b=0.388$ nm, and $c=1.276$ nm) with K_2NiF_4 structure and (00ℓ) bcc α-Fe ($a=0.287$ nm). This result shows that in the absence of oxygen the $La_{0.5}Sr_{0.5}FeO_3$ target phase does not grow homogeneously as a single-phase film, but spontaneously decomposes into a two-phase state that consists of $LaSrFeO_4$ and α-Fe. Both phases are highly crystalline, and (001) oriented. The cross-sectional TEM image of the film grown at $T=760\ ^\circ\mathrm{C}$ [Fig. 1(b)] shows that the α-Fe phase is embedded in the $LaSrFeO_4$ matrix. The secondary α-Fe phase grows perpendicular to the surface of the substrate and forms single crystalline nanowires. The in-plane epitaxial relationship of the two phases obtained from plan view electron diffraction[2] indicates that the α-Fe second phase is rotated 45° with respect to the $LaSrFeO_4$ lattice so that $[110]_{\alpha\text{-Fe}}\|[100]_{\mathrm{LaSrFeO_4}}$ and $[100]_{\alpha\text{-Fe}}\|[110]_{\mathrm{LaSrFeO_4}}$.

Figures 2(a)–2(c) shows plan view TEM images of the nanowires grown at different temperatures. It can be seen that the lateral dimensions of the α-Fe nanowires are strongly dependent on growth temperature. By reducing the temperature of deposition, the size and spacing between the iron nanowires decrease. The insets to the figures show statistical size distributions of the nanowires grown at $T=840\ ^\circ\mathrm{C}$ [Fig. 2(a)], $T=760\ ^\circ\mathrm{C}$ [Fig. 2(b)], and $T=560\ ^\circ\mathrm{C}$ [Fig. 2(c)] which fit a Gaussian distribution with mean diameters of $d=50$, 16, and 4 nm, respectively. It also shows that for the nanowires grown at $T=760$ and 560 °C, 95% of the nanowires are within the size range of $d=15-20$ nm and $d=3-6$ nm, respectively. For the samples grown at $T=840\ ^\circ\mathrm{C}$, the size distribution of the second phase is slightly larger and 85% of the pillars are within the size range of $d=45-55$ nm.

It is evident that at lower deposition temperatures, since the mobility of the atoms is low and the diffusion length is short, the nucleation of many small iron second phase sites is favored. At higher deposition temperature the atoms become more mobile and the surface diffusion becomes important resulting in the attachment of Fe atoms to an existing iron second phase nucleus. This leads to the formation of fewer and larger iron second phases. Figure 2(d) shows the temperature dependence of the Fe nanowires' lateral dimensions. It is possible to fit the temperature dependence of the lateral dimensions to an Arrhenius-type behavior yielding an activation energy of $E_v \approx 1.2$ eV for the reduction of $La_{0.5}S_{0.5}FeO_3$

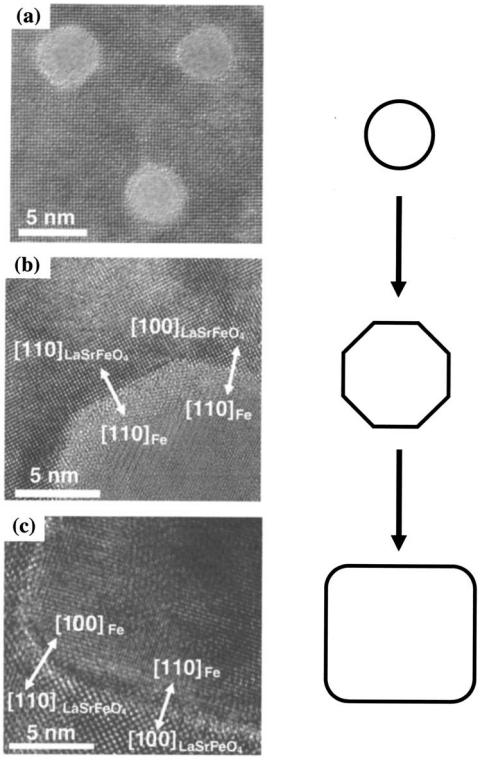

FIG. 3. Plan view high resolution TEM images of (a) circular nanowires grown at $T=560\ ^\circ\mathrm{C}$, (b) a section of nanowires grown at $T=760\ ^\circ\mathrm{C}$ showing the interface between a single Fe nanowire and $LaSrFeO_4$ matrix, and (c) a section of almost square nanowires grown at $T=840\ ^\circ\mathrm{C}$ showing [110] facets of Fe pillars dominating. The schematic of shape changes of nanowires is shown in parallel to high resolution TEM images.

and the formation of the α-Fe nanowires. In addition, we have shown that the volume fraction of the Fe nanopillars in the film equals approximately 10%,[2] and is independent of the deposition temperature. Arrhenius-type behavior of the size evolution of the iron nanowires in addition to constant volume fraction suggests that the growth of the nanowires is kinetically controlled by diffusion during growth.[7,8] This also explains the broadening of the statistical size distribution of the iron second phase at higher growth temperature.[9]

Interestingly the in-plane shape of the nanowires also changes as the temperature of deposition and therefore the size of the nanowires increase. The nanowires grown at temperature around $T=560\ ^\circ\mathrm{C}$ have circular shape with average diameter of about $d=4$ nm, see Fig. 3(a). The shape evolves to octahedral form with only [110] and [100] facets as the temperature of deposition increases. An example is shown in Fig. 3(b) for the film grown at $T=760\ ^\circ\mathrm{C}$. Nanowires with almost square shape form when the deposition temperature is further raised to $T=840\ ^\circ\mathrm{C}$, see Fig. 3(c). The equilibrium shapes are all symmetric with [110] facets dominating.

Here, we first discuss the symmetrical shapes of the iron nanowires and then focus on the temperature dependency of their shapes. The morphologies and symmetry properties of crystals embedded in a crystalline matrix can be explained by the group theory developed by Cahn and Kalonji.[10] In our case, the symmetry point groups for α-Fe (bcc) nanowires and $LaSrFeO_4(K_2NiF_4)$ matrix are $m3m$ and $4/mmm$, respectively. Therefore, with respect to group theory a heterophase interface between α-Fe and $LaSrFeO_4$ phases should belong to a group that contains all the point symmetry elements of both the matrix and the second phase, which is $4/mmm$ in

this case. According to this theory, if the interface point group belongs to $4/mmm$ group the symmetry dictated extremum will exist with [110] and [100] facets parallel to each other. In our experiments with α-Fe nanowires embedded in $LaSrFeO_4$, where symmetrical square-shaped second phase is observed, this extremum is therefore an energy minimum.

The energy of a system containing coherent particles is given by the sum of its surface and elastic energies. Because the ratio of elastic to surface energy for a second phase is proportional to its size, the shape that minimizes the surface energy is stable when the second phase is small and evolves to the shape that minimizes the elastic energy when the precipitate is large.[11] As a result, the evolution of the circular to more faceted shapes occurs as the size of the second phase increases. It is interesting to estimate the diameter of the second phase at which this evolution begins. McCormack, Khachaturyan, and Morris have studied the morphological evolution of a cubic coherent inclusion in a two-dimensional elastic medium,[12] which is equivalent to an infinitely long cylinder with the misfit acting only on the plane perpendicular to the cylinder long axis. In their theoretical calculations, minimization of the sum of both surface energy and elastic strain energy leads to an effective length $r_0=\sigma/4E^*$, which measures the relative contribution of both surface and elastic energies. Here σ is the surface energy and E^* is defined as $E^*=-\beta^2\Delta\varepsilon_0^2/2c_{11}(2c_{11}-\Delta)$, where c_{ii} is the elastic constant, $\Delta=c_{11}-c_{12}-2c_{44}$ is the elastic anisotropy constant, and $\beta=c_{11}+2c_{12}$ is the bulk modulus. We have applied these results to iron nanowires formed by phase decomposition assuming that the principle strain parallel to long axis of nanowires is much smaller than that of perpendicular to long axis. Considering the values available for α-Fe (bcc) with elastic anisotropy constants of $c_{11}=222.7$, $c_{12}=128.7$, and $c_{44}=131.3$ GPa[13] (negative elastic anisotropy) and surface energy $\sigma_s=2.41(\mathrm{J/m^2})$[14] we find that for an in-plane strain of $\varepsilon_{xy}=0.046$ (equal to the lattice mismatch between α-Fe and $LaSrFeO_4$), the minimization of free energy in α-Fe nanowires results in an effective length of $r_0=2$ nm.

The finite element simulation method performed by McCormack and co-workers[12] shows that the circular shape is stable when the cross-sectional length (D) of the second phase is $D<4r_0$. Beyond this diameter the circular nanowires evolve into a more faceted octahedron shape and finally to square shape with elastically soft facets dominating when $4r_0<D<27r_0$. In this study, the circular shape is observed when the diameter of the nanowires is between 3 and 6 nm. Theoretically, the circular shape of iron nanowires should evolve to octahedral or square cross sections when $D>8$ nm. This is confirmed in the film grown at $T=760\ ^\circ$C. Here, octahedral shape with an average diameter around $d=16$ nm and [110] and [100] facets is observed [Fig. 3(b)]. The smallest diameter observed in the films grown at this temperature is around 11 nm [Fig. 2(b)] which shows the same faceting behavior. Thus the transition from circular to octahedral shapes occurs in the region $6<d<11$ nm which is in good agreement with the theoretical values estimated from the model of McCormack and coworkers. The observation of octahedral shape with [110] and [100] facets is due to the anisotropic nature of the surface tension. As the temperature of the deposition and therefore the lateral size of the nanopwires increases, square-shaped nanowires are expected to appear with [110] facets, which tends to be the elastically soft direction in bcc structures. In the present case, even at higher growth temperatures as nanowires of average diameter $d=50$ nm are formed, there are some small [100] facets at the corners of the square as seen in Fig. 3(c). This is due to the fact that in α-Fe with bcc structure the order of the surface free energy is $\sigma_{110}\leqslant\sigma_{100}<\sigma_{111}$, with the surface energies of the [100] and [110] facets very close to each other.[15,16] In some cases the surface energy of [100] is shown to be even slightly higher than [110] facets. This is due to the magnetic energy contribution to the surface energy, which lowers the surface energy of the more open [100] surface in some $3d$ metals including iron.[17]

In summary, ferromagnetic iron nanowires exhibiting three-dimensional heteroepitaxy have been synthesized through phase decomposition. The size evolution of the iron nanowires suggests that the growth of nanowires is kinetically controlled by diffusion during the growth. The symmetric square shape of the iron nanowires with [110] facets of α-Fe parallel to [100] facets of the matrix is energetically favorable at high temperatures and corresponds to that predicted by group theory. The in-plane shape evolution of the nanowires from circular to square cross section takes place as the size of the nanowires increases and elastic energy effects dominate. A fit to the theoretical calculations shows that the circular shape evolves first to an octahedral shape followed by a square shape when the diameter of the nanowires increases beyond 8 nm.

The authors acknowledge the support of the staff and facilities at the National Center for Electron Microscopy. This work was partially supported by University of Maryland NSF MRSEC under Grant No. DMR-00-80008 and ONR under MURI program N000140110761.

[1] J. I. Martín, J. Nogués, K. Liu, J. L. Vicente, and I. K. Schuller, J. Magn. Magn. Mater. **256**, 449 (2003).
[2] L. Mohaddes-Ardabili, H. Zheng, S. B. Ogale, B. Hannoyer, W. Tian, J. Wang, S. E. Lofland, S. R. Shinde, T. Zhao, Y. Jia, L. Salamanca-Riba, D. G. Schlom, M. Wuttig, and R. Ramesh, Nat. Mater. **3**, 533 (2004).
[3] J. M. D. Tascón, J. L. G. Fierro, and L. G. Tejuca, J. Chem. Soc., Faraday Trans. 1, **81**, 2399 (1985).
[4] Y. G. Zhao, Y. H. Li, S. B. Ogale, M. Rajeswari, V. Smolyaninova, T. Wu, A. Biswas, L. Salamanca-Riba, R. L. Greene, R. Ramesh, T. Venkatesan, and J. H. Scott, Phys. Rev. B **61**, 4141 (2000).
[5] H. Zheng, J. Wang, S. E. Lofland, Z. Ma, L. Mohaddes-Ardabili, T. Zhao, L. Salamanca-Riba, S. R. Shinde, S. B. Ogale, F. Bai, D. Viehland, Y. Jia, D. G. Schlom, M. Wuttig, A. Roytburd, and R. Ramesh, Science **303**, 661 (2004).
[6] H. Zheng, J. Wang, L. Mohaddes-Ardabili, D. G. Schlom, M. Wuttig, L. Salamanca-Riba, and R. Ramesh, Appl. Phys. Lett. **85**, 2035 (2004).
[7] M. Meixner, E. Schöll, V. A. Shchukin, and D. Bimberg, Phys. Rev. Lett. **87**, 236101 (2001).
[8] F. Léonard, M. Laradji, and R. C. Desai, Phys. Rev. B **55**, 1887 (1997).
[9] M. Meixner, R. Kunert, and E. Schöll, Phys. Rev. B **67**, 195301 (2003).
[10] J. W. Cahn and G. Kalonji, *Proceedings of an International Conference on Solid-Solid Phase Transformations*, edited by H. I. Aaronson, D. E. Laughlin, R. F. Sekerka, and C. M. Wayman, 1982, p. 3.
[11] W. C. Johnson and J. W. Cahn, Acta Metall. **32**, 1925 (1984).
[12] M. McCormack, A. G. Khachaturyan, and J. W. Morris, Acta Metall. Mater. **40**, 325 (1992).
[13] P. Söderlind, R. Ahuja, O. Eriksson, J. M. Wills, and B. Johansson, Phys. Rev. B **50**, 5918 (1994).
[14] W. R. Tyson and W. A. Miller, Surf. Sci. **62**, 267 (1977).
[15] L. Vitos, A. V. Ruban, H. L. Skriver, and J. Kollár, Surf. Sci. **411**, 186 (1998).
[16] M. J. S. Spencer, A. Hung, I. K. Snook, and I. Yarovsky, Surf. Sci. **513**, 389 (2002).
[17] M. Aldén, H. L. Skriver, S. Mirbt, and B. Johansson, Surf. Sci. **315**, 157 (1994).